Phase stabilities and homogeneity ranges in 4*d*-transition-metal carbides: A theoretical study

Håkan W. Hugosson,[1] Olle Eriksson,[1] Ulf Jansson,[2] and Börje Johansson[1]
[1]*Condensed Matter Theory Group, Department of Physics, Uppsala University, Box 530, S-751 21 Uppsala, Sweden*
[2]*Inorganic Chemistry Group, Ångström Laboratory, Uppsala University, Box 538, S-751 21 Uppsala, Sweden*
(Received 13 October 2000; published 13 March 2001)

First-principles full-potential linear muffin-tin orbital calculations have been used to study the 4*d*-transition-metal carbides ZrC, NbC, and MoC. The experimental phase diagrams at $T=0$ of the refractory compounds ZrC, NbC, and MoC have been reproduced with great accuracy from first principles theory. The energy of formation for these compounds has been calculated for several phases and stoichiometries in order to understand the differences in phase stabilities and the changes in homogeneity ranges found between these systems is explained. The results can be regarded as theoretical zero-temperature phase stability diagrams for the three compounds containing not only the experimentally verified but also hypothetical phases and many of the experimental properties and trends are reproduced and explained. A study of the changes and differences in electronic structure and bonding of the studied compounds, phases and stoichiometries is also presented. As a part of this study the hexagonal Me_2C (Me being Zr, Nb, or Mo) phases were studied and the theoretical structures, with relaxed interlayer distances and lattice parameters, were obtained. The phase stabilities and electronic structure of the experimentally reported orthorhombic Nb_2C and Mo_2C phases were also studied.

DOI: 10.1103/PhysRevB.63.134108 PACS number(s): 64.60.My, 71.15.Nc, 71.20.Be

I. INTRODUCTION

Several semiempirical methods exist to construct phase diagrams based on approximate free energy functions fitted to existing thermodynamic data. Though these methods are all very useful it would be even more useful, and scientifically more gratifying, to obtain phase diagrams and thermodynamic functions strictly from knowledge of the constituent atoms. Such a first principles approach to calculating the phase diagrams of compounds has long been a sought after goal for theoreticians and provides enormous challenges. In order to calculate phase equilibria the Gibbs free energy must be known for the competing structures over a wide range of concentrations. The energies of formation for a large number of phases over a range of stoichiometries need to be determined. A technologically attractive and theoretically challenging group of compounds with consistent trends yet significant differences in the phase diagrams are the transition metal carbides. This class of materials is an important testing ground for theoretical first principles calculations of phase diagrams since they are particularly complex to describe theoretically. This complexity is due to the presence of vacancies, difficult to treat accurately with most available methods, and in addition the bonding characteristics are diverse.

The transition metal carbides have a unique combination of properties, e.g., high hardness, high melting point, and excellent electrical conductivity, making them suitable as bulk or thin film materials in many technological applications. Today, a large number of transition metal carbide phases is known. However, thermodynamically stable binary carbides are only formed by the transition metals in groups IV, V, VI and by Mn in group VII. From a structural point of view, most of these carbides (except chromium carbides) can be described as a stacking of close-packed metal layers with carbon interstitial sites between the metal planes. As one moves across the Periodic Table, the structure of the carbide phases will change. The group IV carbides (TiC, ZrC, and HfC) only crystallize in the cubic NaCl structure. This structure is also found among the group V metals (V, Nb, and Ta) but in this group, hexagonal Me_2C phases are also formed at lower carbon contents. In contrast, the group VI metals (Cr, Mo, and W) can form several different carbide phases. At the same time the experimental phase diagrams of the group IV, V, and VI transition metal carbides show many similarities. In Fig. 1 we show the phase diagrams of ZrC, NbC, and MoC.[1] In all three groups one finds a substoichiometric cubic phase where the composition is varied by changes in the occupancy of carbon atoms in the interstitial sites. A general rule seems to be that the width of the homogeneity range of the cubic phase decreases when going from the group IV to the group VI metals. This is well illustrated by comparing the phase diagrams of ZrC and δ-MoC. While both exhibit the NaCl structure, ZrC has a fairly wide homogeneity range varying from about $ZrC_{0.45}$ to $ZrC_{0.95}$, whereas the δ-MoC phase has a much more narrow composition range varying from about δ-$MoC_{0.66}$ to δ-$MoC_{0.75}$. To understand this difference in homogeneity ranges one must study the energies of formation of the competing phases found in the transition metal carbides. Combining the information from the phase diagrams of the three groups one finds that there are, at least, four competing phases at 50% carbon content; the cubic NaCl phase and in MoC three additional competing hexagonal phases termed γ (WC), γ' (TiAs),[2] and η. The substoichiometric cubic carbides form in the carbon content range of 33% to 50%. At 33% several competing Me_2C phases have been verified, and a high temperature hexagonal structure is followed first by a more stable hexagonal and then a low temperature orthorhombic structure. A general feature seems to be that these Me_2C phases compete with the substoichiometric cubic phase and that the Me_2C phases define the lower limit of the homogeneity range for the substoichiometric cubic phase. The high temperature hexagonal Me_2C phase crystallizing in the ϵ-Fe_2N type structure is common

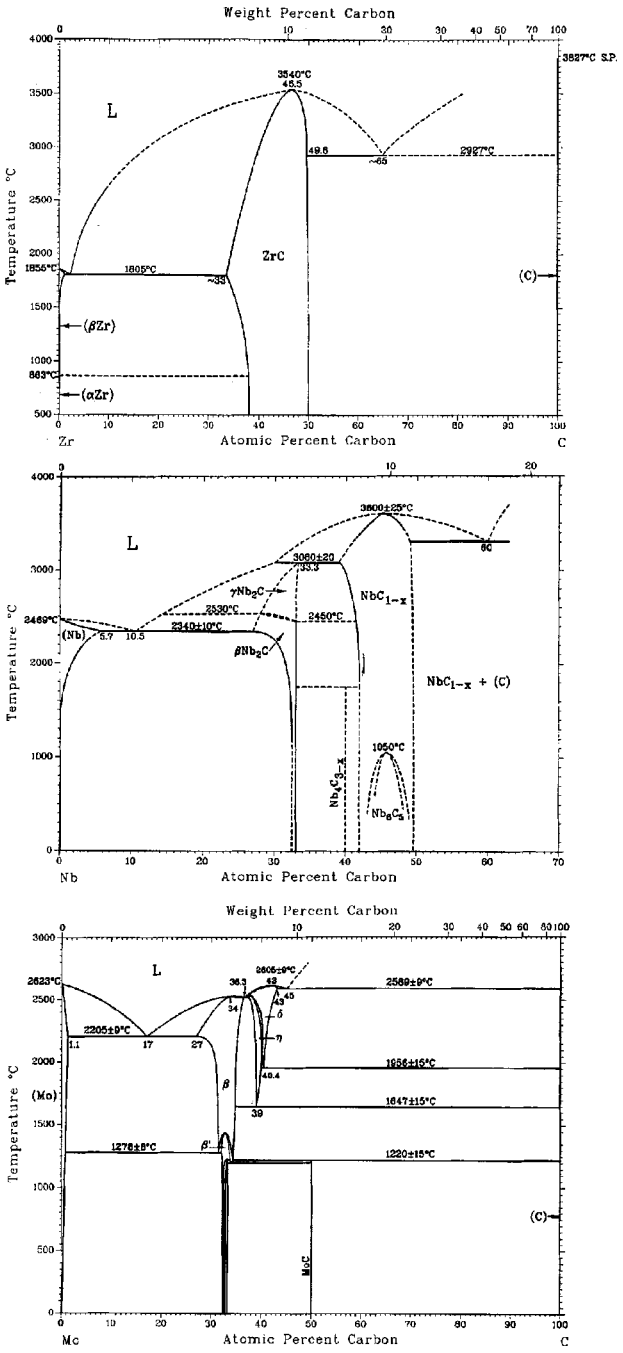

FIG. 1. Experimental phase diagram for the Zr-C, Nb-C, and Mo-C systems (Ref. 1). Stoichiometric and substoichiometric ZrC forms in the cubic NaCl structure. Stoichiometric and substoichiometric NbC forms in the cubic NaCl structure, while γ and β-Nb_2C are hexagonal phases. Stoichiometric MoC forms in the hexagonal WC structure, while δ-MoC is the NaCl structure and η-MoC is a second hexagonal structure. The β and β'-Mo_2C are hexagonal phases.

to both the $4d$ (among them Nb and Mo) and the $5d$ (among them W) transition-metal hemicarbides.

Given the technological interest in transition-metal compounds and the large experimental activity many theoretical calculations have been made on these systems using a wide variety of techniques. Early work in this field is summarized in two review articles by Calais[3] and Neckel[4] and two later comprehensive reviews of the field are due to Schwarz[5] and Johansson.[6] A study of the relative phase stabilities between the cubic NaCl structure and the hexagonal WC structure in the TiC and WC system has been made by Price and Cooper.[7] Theoretical calculations of substoichiometric compounds have been done on cubic MoC_{1-x} by Ivanovskii and co-workers[8] using a Green's function LMTO method and by Krainik *et al.* using a LCAO-CPA method.[9] Theoretical studies of other substoichiometric transition metal carbides include work on TiC using the APW method by Redinger and co-workers[10,11] and studies of the elastic and thermal properties by Wolf and co-workers.[12] Substoichiometric TiX and VX; X=C, N, O, has been studied by Ivanovskii and co-workers using a LMTO-Green's function method.[13] Hugosson and co-workers have also previously reported a study on the effect of vacancies on the relative phase stability of the four experimentally verified MoC phases.[14] Previous attempts at determining the phase stabilities and phase diagrams have been limited to the effective cluster interactions for single phases[15] or to systems with simpler metallic bonding such as FeCr.[16]

The object of the present study is to explain similarities and differences in the phase diagrams of the group IV, V, and VI transition metal carbides by calculating the energy of formation of several competing phases and to gain additional insight about the bonding in these compounds by studying the differences and changes in the electronic structure of the phases. This has been done for the $4d$-transition-metal carbides in a wide range of carbon content using a full-potential all-electron method thereby obtaining what one can regard as theoretical zero-temperature phase stability diagrams containing not only the experimentally verified phases but also the pertinent hypothetical phases. In order to obtain the full phase diagram additional phases should be taken into account and the temperature effects must included, but this has been outside the scope of the present study.

The paper starts with the method and setup of the structures in Sec. II, in Sec. III the energy of formation and equilibrium volumes for the different structures are presented finally leading up in Sec. IV to a theoretical zero temperature phase diagram. In Sec. VI the electronic structure of the different phases is examined and contrasted. The article is ended with a brief conclusion and discussion of the results.

II. METHOD AND SETUP

The calculations presented have been made using a full-potential linear muffin-tin orbital method (FP-LMTO) within the local density approximation (LDA) of density functional theory (DFT).[17,18] The function used for the exchange correlation has been the Hedin-Lundqvist parametrization.[19] In the FP-LMTO method the unit cell is divided into nonoverlapping muffin-tin spheres, inside of which the basis functions are expanded in spherical harmonics up to a cutoff in angular momentum, $l_{max}=6$. The basis functions in the interstitial region, outside the muffin-tin spheres, are Neumann or Hankel functions. This division of space implies that one must take care to use the same ratio of muffin-tin

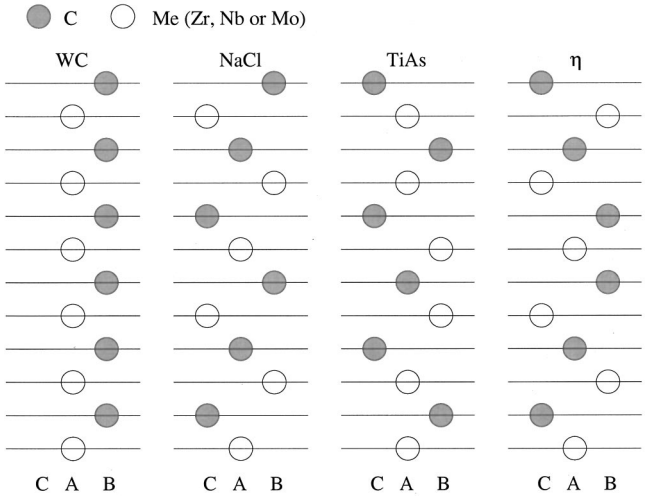

FIG. 2. Structures of the stoichiometric MeC (Me being Zr, Nb, or Mo) transition metal carbide phases studied. They are shown here as variations in stacking sequence of close-packed-like planes of metal and carbon atoms.

volume versus interstitial volume in order to compare energies between several phases with varying degrees of packing. To speed up convergence each eigenvalue is convoluted with a Gaussian with a width of 20 mRy.[20] Energy convergence in terms of the number of **k** points has also been reached so that this has a minimal effect when comparing energies of different structures and compounds. When describing the atoms of the crystal the electronic states are divided into core, pseudocore, and valence states. For the transition metal atoms the $5s$ and $4d$ states were treated as valence states while the $4p$ and $4s$ states were treated as pseudocore. The pseudocore and valence states were allowed to hybridize in one common energy panel. In the carbon atom the $1s$ level was treated as a core state while the $2s$ and $2p$ levels were treated as valence states. To find the final equilibrium energies the carbon basis set was extend to include also $3d$ orbitals. This lowered the ground-state energies while it did not influence the equilibrium volumes.[21]

All the structures were relaxed in the lattice parameter a and, for the WC, η and TiAs structures also in c. Local relaxations around the impurity atoms have not been taken into account here, such a relaxation is likely to lower the equilibrium energies somewhat.[22] The total energy vs volume was calculated for several, from 6 to 9, volumes in each structure and stoichiometry and the resulting energy versus volume curves were fitted to a Murnaghan equation of state to find the theoretical ground state energies, and equilibrium volumes.

Several phases and stoichiometries were investigated and a total of 13–14 structures were studied for all three transition metal compounds, ZrC, NbC, and MoC. In the case of 50% carbon content the cubic NaCl structure and the hexagonal WC, TiAs, and η-MoC phases were studied. For 0% carbon the metal bcc and fcc structures were studied for Nb and Mo and for Zr also the hcp structure. A presentation of the geometric structures of the MeC phases is given in Fig. 2. The WC phase has a hexagonal structure with an experimental axis ratio $c/a=0.969$. The TiAs and η structures are also hexagonal with $c/a=3.741$ and $c/a=4.86$. The fourth structure is the well-known cubic NaCl structure with an fcc Bravais lattice. For the Me_2C phases the hexagonal phase has been chosen as a model structure for all three Me_2C compounds while the orthorhombic Nb_2C and Mo_2C structures have also been studied for sake of completeness.

III. ENERGIES OF FORMATION AND EQUILIBRIUM VOLUMES

In order to study the relative phase stabilities the energy of formation, E_{form}, needs to be calculated for the structures and stoichiometries studied. The energy of formation per atom is defined as

$$E_{\text{form}}=\frac{E(Me_mC_n)}{n+m}-\frac{mE(Me)}{n+m}-\frac{nE(C_{\text{graphite}})}{n+m}, \quad (1)$$

where n and m are the number of atoms used in the supercell and with the energy of the metal being calculated in the bcc phase for Nb and Mo, and in the hcp phase for Zr (and Tc).

For ease of discussion in the coming sections, changes that decrease the energy of formation (thus increasing the stability) for a compound or structure will be described as stabilizing. For example, if NbC is found to be more stable (having a higher heat of formation) than ZrC for a given structure, then the electronic states that are filled in NbC will be denoted as being stabilizing. The description of electronic states as stabilizing/destabilizing is thus analogous to the notation bonding/antibonding states commonly used when discussing cohesive energies. When discussing bonding/antibonding states the electronic states of the parent atoms are used as references while the notation stabilizing/destabilizing states use the electronic states of the parent solids as references. The distinction into stabilizing/destabilizing states is made in order to identify changes in the electronic structure that lead to a stabilization of a compound or structure, something that an increase in the cohesive energy in itself does not uniquely indicate.

A. Stoichiometric MeC phases

In the case of MoC no less than four competing MeC phases are experimentally found, while this is not the case for ZrC and NbC were the only experimentally verified phase is the cubic NaCl phase. Furthermore the stable stoichiometric MoC phase is the hexagonal γ (WC) phase. To understand more about the competition between the phases the energy of formation has been calculated for the four MoC phases in all three compounds. The formation energies and equilibrium volumes of these phases and all the other phases studied in the present work are collected in Table I. From an inspection of the energies of formation of the stoichiometric structures a drastic change in the relative order of stability is found to occur between NbC and MoC, where the cubic phase ceases to be the most stable. In order to further ascertain this trend, highly hypothetical, TcC in the cubic NaCl and hexagonal WC structures have also been studied. From the changes in the formation energy it is found that the

TABLE I. Number of atoms in structure, equilibrium volumes V_{eq}, and formation energies E_{form} for all the phases studied.

Phase	Atoms	V_{eq} [Å^3]	E_{form} [mRy]
Zr(hex)	1	22.0	0
Zr(bcc)	1	21.2	5
Zr(fcc)	1	21.8	4
ZrC (NaCl)	2	25.3	-67
ZrC (WC)	2	26.0 (Ref. 34)	-6
ZrC (TiAs)	8	24.7 (Ref. 34)	-37
ZrC-η	12	25.2 (Ref. 34)	-59
$ZrC_{0.875}$	15	25.0	-63
$ZrC_{0.75}$	7	25.0	-53
$ZrC_{0.75}$	14	24.8	-58
$ZrC_{0.50}$	6	24.5	-36
$ZrC_{0.50}$	12	24.3	-46
$ZrC_{0.25}$	5	23.6	-18
Zr_2C (hex)	3	24.9	-44
Nb(bcc)	1	17.2	0
Nb(fcc)	1	17.9	29
NbC (NaCl)	2	21.9	-43
NbC (WC)	2	20.4 (Ref. 34)	-9
NbC (TiAs)	8	21.3 (Ref. 34)	-25
NbC-η	12	21.9 (Ref. 34)	-41
$NbC_{0.875}$	15	21.6	-43
$NbC_{0.75}$	7	21.4	-33
$NbC_{0.75}$	14	21.3	-42
$NbC_{0.50}$	6	20.7	-22
$NbC_{0.50}$	12	20.6	-27
$NbC_{0.25}$	5	19.7	-3
Nb_2C (hex)	3	20.6	-37
Mo(bcc)	1	15.2	0
Mo(fcc)	1	15.4	32
MoC (NaCl)	2	20.3	10
MoC (WC)	2	20.3 (Ref. 34)	-11
MoC (TiAs)	8	20.3 (Ref. 34)	5
MoC-η	12	20.2 (Ref. 34)	9
$MoC_{0.875}$	15	19.9	4
$MoC_{0.75}$	7	19.4	5
$MoC_{0.75}$	14	19.4	-1
$MoC_{0.50}$	6	18.5	4
$MoC_{0.50}$	12	18.3	-6
$MoC_{0.25}$	5	17.3	14
Mo_2C (hex)	3	18.6	-6
Mo_2C (ortho)	12	18.3	-12
Tc (hex)	1	13.8	0
TcC (NaCl)	2	19.6	43
TcC (WC)	2	19.2	3

effect of band-filling is that that the WC structure is slightly stabilized (E_{form} is fairly constant) up to MoC and then destabilized (E_{form} increases) up to TcC. The electronic states that are filled in the WC structure are thus slightly stabilizing up to MoC and then destabilizing. In the other three structures the effect of band-filling when traversing the series from ZrC to TcC is destabilizing. The WC structure therefore becomes the most stable structure for MoC not by becoming more stable in itself but because the other phases are destabilized. The difference in energies of formation between the structures is the smallest for MoC. This span in energy of formation indicates how easily the less stable phases may be formed and a small span shows why MoC has so many stable and meta-stable phases while the other transition metal carbides do not.[23]

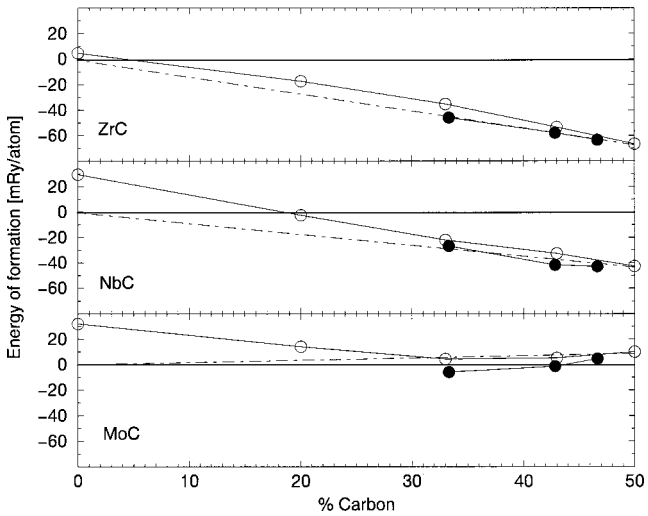

FIG. 3. Energies of formation for substoichiometric cubic ZrC_{1-x}, NbC_{1-x}, and MoC_{1-x} shown as a function of carbon content. The results from the 8 atom supercell are indicated by circles and the results from the 16 atom supercell by the filled circles. The dash-dotted lines indicates the energy of formation of the stoichiometric cubic phases plus the pure metal phase.

B. Substoichiometric cubic MeC_{1-x}

The cubic phases of ZrC, NbC, and MoC were studied over a wide range of vacancy concentration, from MeC to Me (fcc) first using a supercell setup with a simple cubic lattice with a basis of 4 transition metal atoms and 4 carbon atoms. The carbon atoms were subsequently removed one by one creating $MeC_{0.75}$, $MeC_{0.50}$, $MeC_{0.25}$ and finally fcc Me. The substoichiometric cubic phase was also studied using a larger supercell with an fcc lattice and a basis of 8 transition metal atoms and 8 carbon atoms to allow for a larger and different choice of stoichiometries and vacancy positions.[24]

The equilibrium volumes and energies of formation, E_{form}, of the different phases and stoichiometries are presented in Fig. 3 and collected in Table I. The difference between the two supercells used, 8 atoms and 16 atoms, is significant. In the larger supercell one can spread out the vacancies more evenly in the structure, thereby minimizing the number of metal atoms with more than one carbon vacancy neighbor, while this is not possible in the smaller supercell. This is seen to have a large effect on the total energy of the system and the stability trends. The smaller supercell should, however, be more representative when the vacancy concentrations are large, like in $MoC_{0.25}$, where nearly all the carbon atoms have been removed.

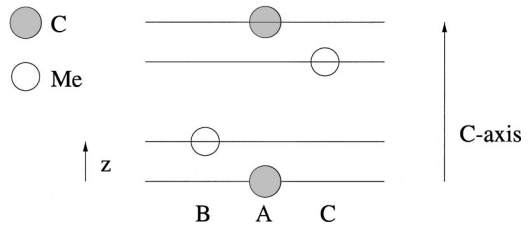

FIG. 4. Structure of the hexagonal Me_2C phases, Me being Zr, Nb, or Mo, showing the *c*-axis and the layer distance *z* which is relaxed.

The energies of formation for the substoichiometric cubic carbides are seen to be very different in the three compounds. For ZrC_{1-x} the energy of formation, E_{form}, is negative almost over the whole region, in NbC_{1-x} it is so above 20% carbon content while the E_{form} of MoC_{1-x} is negative between 33% and 43% carbon content. Comparing the E_{form} of the substoichiometric carbides against that of the respective stoichiometric carbide plus the pure metal it is seen that ZrC_{1-x} is stable down to $ZrC_{0.50}$ while NbC_{1-x} is not stable for $NbC_{0.50}$. Cubic MoC_{1-x} is more stable than cubic MoC plus bcc-Mo down to around 33% carbon.

Figure 3 also clearly shows the very different behavior of the three compounds when vacancies are introduced into the supercell. In ZrC_{1-x} the energy of formation increases when vacancies are introduced while for NbC_{1-x} the energy of formation, E_{form}, decreases or is unchanged for the first two stoichiometries and then increases. For MoC the change is negative until $MoC_{0.50}$. This is a clear indication that the states which are being unoccupied by the removal of carbon atoms are of a very different nature in ZrC, NbC, and MoC. All the states removed in ZrC are stabilizing states while for MoC one is first removing non-stabilizing or destabilizing states, until below 33% carbon content. In NbC one first removes destabilizing states and then stabilizing states.

C. Equilibrium structures of hexagonal Me_2C

The hexagonal Me_2C (Me = Zr, Nb, and Mo) phases presents a challenge since for the group IV transition metals this phase is not found experimentally and for MoC and NbC several competing Me_2C phases exist. In our study the hexagonal Nb_2C structure, also found as a high temperature phase in Mo_2C and W_2C, was used as a model structure for the Me_2C phases even if this is not the equilibrium structure for all three compounds. In the Me_2C phases the distance between the layers of the carbon atoms and metal atoms, here called *z* (see Fig. 4), is not known experimentally for Zr_2C, since it has never been synthesized. Therefore the equilibrium structures, interlayer distances and lattice parameters have been calculated theoretically using relaxations of the structures with quantum mechanical forces. The same ratio of $c/a = 1.566$, from Mo_2C, was used for all phases.[25]

First a model structure of the hexagonal Me_2C phases was studied by using the layer distance $z = 0.25c$ and the equilibrium lattice constant was found from this setup. The layer distance was then allowed to relax for this preliminary equilibrium lattice constant, this new layer distance was then used in a new search for the equilibrium lattice constant. The result was, however, that for some lattice constants the original guess of $z = 0.25c$ had a lower total energy than the structure with ''relaxed'' layer distance. The total energies of the systems were thus found to be very sensitive to the layer distances. Layer distance relaxations, using forces implemented in the FP-LMTO method,[17] were therefore performed for all lattice parameters when searching for the equilibrium energy and volume in each compound. The layer distance was found to be strongly dependent on the lattice parameter indicating that the actual bond distance between the atoms in these compounds is important. The equilibrium volumes, layer distances *z* and formation energies for the fully relaxed hexagonal Me_2C structures are collected in Table II. The theoretical lattice parameters agree well with the experimental lattice parameters in those compounds where they are known.[26] Since the interlayer distances are not known experimentally for Zr_2C the values given here are predictions. The stability of the Me_2C carbides decreases when going from Zr_2C to Mo_2C, most drastically between Nb_2C and Mo_2C, showing that the electronic states that are being filled are less bonding than the states of the individual solids.

TABLE II. Experimental and theoretical lattice parameters, theoretical layer distances, and energies of formation for the Me_2C phases.

Phase	a_{expt} [Å]	a_{theor} [Å]	z_{expt} [Å]	z_{theor} [Å]	E_{form} [mRy]
Zr_2C		3.32		1.23	-44
Nb_2C	3.13	3.12	1.23	1.22	-37
Mo_2C	3.02	3.00	1.18	1.19	-6

D. Orthorhombic Nb_2C and Mo_2C phases

The orthorhombic structures of Nb_2C and Mo_2C have also been investigated. The lattice parameter *a* was varied in order to find the equilibrium structure and energy while the experimental b/a and c/a ratios were used.

In the case of Nb_2C some controversy exists as to the determination of the structure of the orthorhombic phase.[27] Two of the reported orthorhombic structures have been studied and compared with the hexagonal phase. The result is, however, that both reported orthorhombic structures are found to have higher energies of formation, thus being less stable, than the hexagonal Nb_2C phase. The result for Mo_2C is that the orthorhombic structure is more stable than the hexagonal phase and stable versus cubic MoC plus bcc Mo, in agreement with experimental reports. The theoretical values for the $a = 4.711$ Å, $b = 5.988$ Å, and $c = 5.185$ Å axes are also in good agreement with experimental results.[28]

IV. THEORETICAL ZERO TEMPERATURE PHASE STABILITY DIAGRAMS

Combining all the hitherto calculated energies of formation one can derive theoretical zero temperature phase stabil-

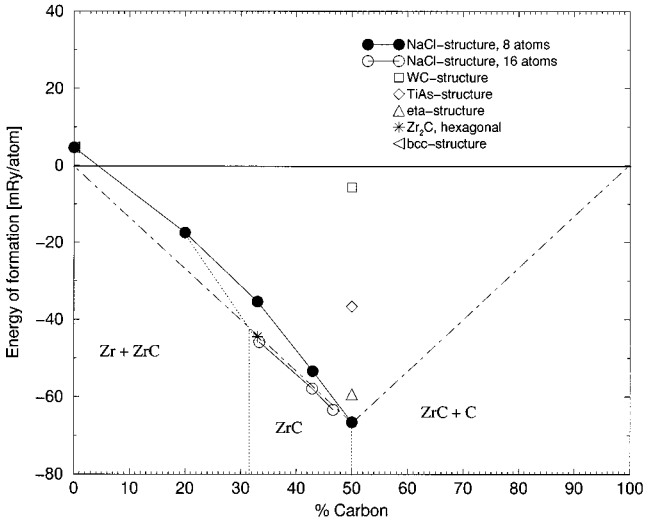

FIG. 5. Theoretical zero temperature phase diagram for ZrC. The dash-dotted lines indicates the energy of formation of the stoichiometric cubic phases plus the pure metal phase (or the carbon graphite phase). Dotted line indicate the approximate phase regions at 0 K.

ity diagrams for ZrC, NbC and MoC and they are displayed in Figs. 5–7. The theoretical phase stability diagrams can be compared with the experimental phase diagrams in Fig. 1 to shed more light upon the experimental results. From the theoretical phase stability diagrams one can extract much of the phase stabilities and trends seen in the experimental phase diagrams. All the phases are collected here, the whole range of carbon content is shown and the energies of the most stable stoichiometric phases plus the pure metal phase (or carbon graphite phase) is indicated by dot-dashed lines.

Starting with the phase stability diagram of ZrC, in Fig. 5, the NaCl structure is predicted to be the stable stoichiometric compound and substoichiometric ZrC_{1-x} is stable compared to the competing phases down to at least 33% carbon. If the energy of formation is extrapolated towards the point for

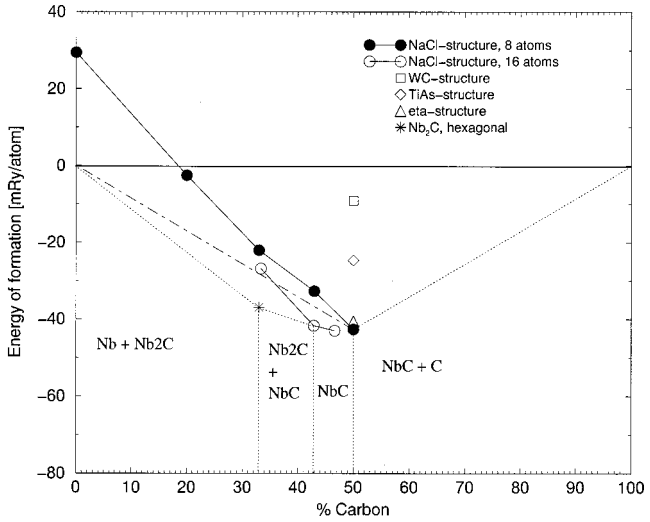

FIG. 6. Theoretical zero temperature phase diagram for NbC. The key to this figure is the same as in Fig. 5.

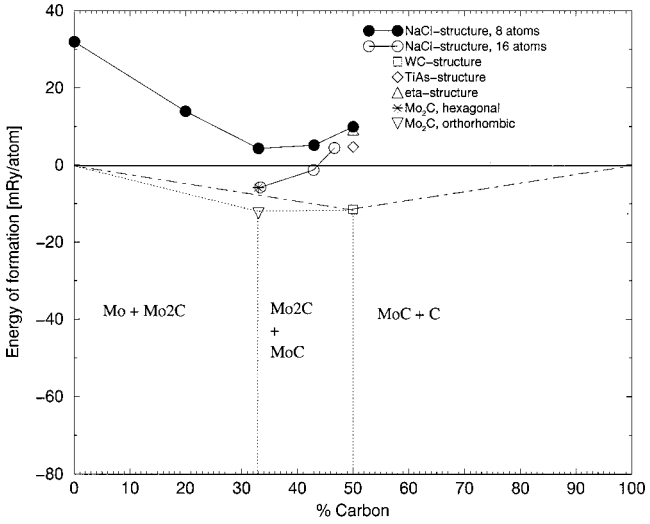

FIG. 7. Theoretical zero temperature phase diagram for MoC. The key to this figure is the same as in Fig. 5.

20% the stability range is predicted to be from 50% carbon down to 32% which is in excellent agreement with experiment. The hexagonal Zr_2C phase is less stable than substoichiometric ZrC_{1-x} which is also in agreement with experiment since the Zr_2C phase is not observed. The phase stability diagram of NbC, Fig. 6, also predicts the correct stable NbC phase, being the NaCl structure, but here the behavior of the substoichiometric phase is somewhat different to that of ZrC_{1-x}. Substoichiometric NbC_{1-x} is seen to be stable versus stoichiometric NbC plus Nb (bcc) only down to 35% carbon and stable versus hexagonal Nb_2C only down to 38% carbon (indicated in the figure with a dashed line). MoC in Fig. 7 shows yet another picture of phase stabilities with a stable WC structure and a substoichiometric cubic structure that is unstable over the whole range of carbon content, in accordance with experiment. It has been shown in previous work that the inclusion of vacancies into the WC structure drastically reduces the stability of this phase having the effect that at substoichiometric compositions the NaCl phase is the most stable.[14] The hexagonal Mo_2C phase is also seen to be unstable while orthorhombic Mo_2C is very stable. Thus only orthorhombic Mo_2C and MoC in the WC structure are stable while the substoichiometric cubic phase is unstable, this all being in agreement with the experimental situation.

The variation in the homogeneity range of the substoichiometric cubic carbides can thus be understood from these phase stability diagrams as arising from the differences in electronic structure with the deoccupation of stabilizing and destabilizing electronic states when vacancies are introduced to the structure. These differences couple into two separate mechanisms stemming from either a competition between the substoichiometric cubic phase and the Me_2C phases plus graphitic carbon or from a competition with stoichiometric cubic MeC plus pure metal Me. The range where the substoichiometric carbide is more stable than both these competitors determines the homogeneity range.

In the figures the regions of solid solution at zero temperature have been indicated by dotted lines. Comparing the

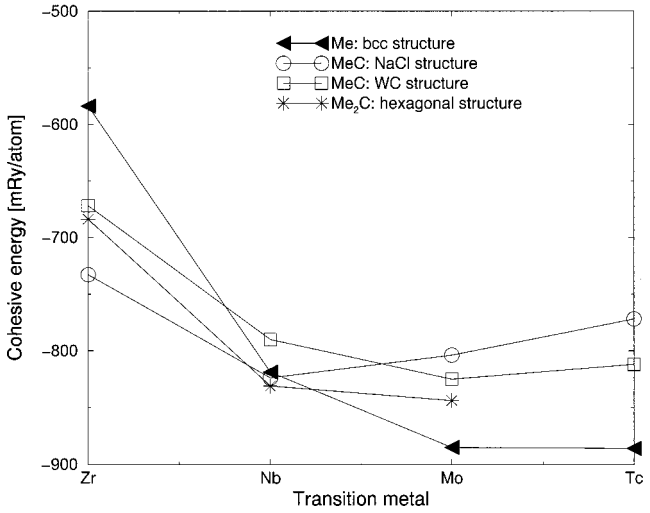

FIG. 8. Cohesive energies for the bcc metals, MeC in WC and NaCl structures and for the hexagonal Me_2C phases.

theoretical regions from Figs. 5–7 with the experimental regions in Fig. 1 it is seen that the experimental situation is perfectly reproduced by the theoretical calculations. The equilibrium composition is also seen to vary, ZrC_{1-x} is seen to be most stable in the stoichiometric composition[29] whereas both NbC_{1-x} and MoC_{1-x} are seen to have minima in E_{form} situated at a vacancy concentration not equal to zero. The equilibrium carbon content for MoC_{1-x} is seen to be around 40% carbon and for NbC_{1-x} it is seen to be around 46% carbon. Concerning the stabilities of the hexagonal Me_2C phases the figures show that Mo_2C and Zr_2C are not stable, while Nb_2C is seen to be stable. This is in accordance with the phase diagrams since Zr_2C is not found experimentally. For hexagonal Mo_2C this instability can be explained since experimentally this is a high temperature structure of Mo_2C, the stable structure for Mo_2C being an orthorhombic structure which is also seen to be stable according to our calculations.

V. COHESIVE ENERGIES

The stability range of the various compounds is determined from a competition between the chemical binding of the pure elements, i.e., graphite (a covalent sp^2 bonded material) and a transition metal (where the bonding is determined by the Friedel model), and the binding in the MeC phase and the Me_2C phase. In order to analyze the nature of the chemical bonds in the latter types of systems we display in Fig. 8 the cohesive energies (E_c) of the MeC compounds in the NaCl and WC structure, the pure elements in the bcc structure and of the Me_2C phases. Several conclusions may be drawn from this figure. First we note the well established fact that for the pure elements a parabolic behavior is observed.[30] For the pure elements, Zr, Nb, and Mo, the electron states are bonding, and the transition from bonding to antibonding states is known to lie close to the electron filling of Tc. For the NaCl compounds the trend is different mainly due to the bonding part of a strong covalent C-*p* Me-*d* hybrid that is just filled in ZrC.[2] The strong binding this results in shows up in a considerably larger value of E_c for ZrC in the NaCl phase compared to the value of the pure element, which explains the large value of the heat of formation for this compound. However, E_c is actually a little larger for NbC, where the extra cohesion comes mostly from metallic bonding of the Nb *d*-states. This is in accordance with previous analysis, since the bonding in NaCl transition metal carbides is composed of metallic *d*-binding in addition to a stronger covalent contribution from the *p*-*d* hybridization.[31] Additional electron filling corresponding to antibonding states and E_c drops in value for MoC and TcC. This picture is somewhat modified for the compounds when they are in the WC crystal structure, since E_c is here actually maximized for MoC and the general trend of the cohesive energy is quite similar to the tend of the pure elements. This suggests a more metallic nature of the chemical bonds in this structure, and the electronic structure[14] is indeed consistent with this. In passing we note that an inspection of the trends of E_c, to identify the transition from bonding to antibonding states, is in some cases dependent on the crystal structure. However, irrespective of this dependence one may note that the transition from bonding to antibonding states lies earlier in the series for the transition metal carbides, compared to the pure elements, a finding that is in accordance with the analysis of Brooks on the chemical binding of the actinide carbides.[32] This is a direct effect of the hybridization between metallic *d* and carbon *p* states.

VI. ELECTRONIC STRUCTURE

The density of states (DOS) is an important quantity for understanding the bonding in a compound. From the characteristic features of the density of states one can understand differences in the chemical bonding between different phases and the changes in the bonding between stoichiometric and substoichiometric phases. A detailed study of the bonding and changes in the bonding is also made by studying the charge density distribution in the compounds and the changes in this distribution coming from the occupation or deoccupation of states in different energy ranges.

A. DOS of stoichiometric MeC phases

The partial DOS for the four structures studied are shown in Fig. 9. For ease of discussion, we can divide the DOS of all four structures into three main regions: (I) a region of predominantly carbon *s* states with a small degree of hybridized *d* states from the transition metal containing 2 states, (II) a region of hybridized carbon *p* states and transition metal *d* states containing 6 states, and (III) predominantly transition metal *d* states with a small degree of hybridized *p* states from carbon, containing 10 states. Region II is usually viewed as the bonding part of the Mo-*d* C-*p* hybridization complex, while region III is the corresponding nonbonding/antibonding part overlapping with metallic *d*-states. The difference between the three compounds is qualitatively, in all four cases, a difference in band-filling where simple rigid band arguments explain the raising of the Fermi level when going from ZrC to MoC. This is also expected and has been

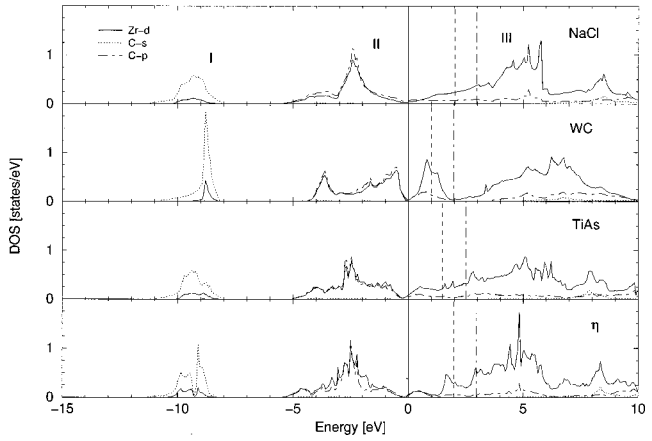

FIG. 9. Density of states for the cubic NaCl (top), hexagonal WC, hexagonal TiAs and hexagonal η-structures (bottom) for ZrC. The Fermi level is indicated by a solid line. The approximate position of the Fermi level for NbC_{1-x}, indicated by a dashed line, and of MoC_{1-x}, indicated by dot-dashed line, is also shown.

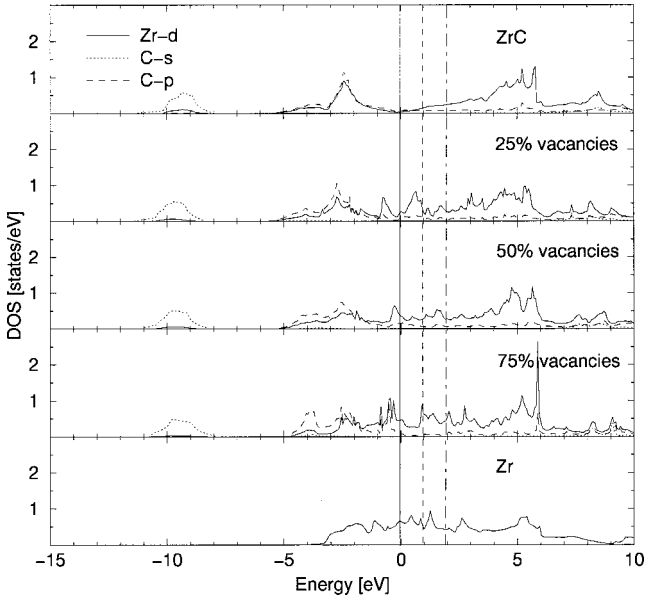

FIG. 10. Density of states for substoichiometric cubic ZrC_{1-x}. The Fermi level is indicated by a solid line. The approximate position of the Fermi level for NbC_{1-x}, indicated by a dashed line, and of MoC_{1-x}, indicated by dot-dashed line, is also shown.

shown to be the case for transition metal substitutions in earlier works.[33] The figures indicate the Fermi level for the ZrC phase by a solid line and the qualitative position of the Fermi level for NbC is indicated by a dashed line and the Fermi level for MoC by a dot-dashed line.

In the topmost part of Fig. 9 the DOS is shown for the cubic NaCl structure. Returning to the discussion regarding the energy of formation of the substoichiometric cubic carbides one can find an explanation of the trends in the electronic structure. In NbC and MoC states in region III are becoming filled. These states are of a very different nature compared to the states in region II which are hybridized carbon *p* states and transition metal *d* states. Using a simple rigid band picture the first electron removed in NbC, going from NbC to $NbC_{0.75}$, is destabilizing where after the states, like in ZrC, are stabilizing. For cubic MoC the first two electrons removed are destabilizing, even though the picture of rigid bands is over simplified it indicates the correct trends.

In order to understand the different behavior as regards the relative phase stabilities for the four structures one must find the difference in the states being filled when going from ZrC to MoC. In ZrC, for all four structures, the Fermi level is in a local minimum of the DOS, a pseudogap, just having filled the 6 states in region II. The largest difference between the four structures is that in the WC structure a fairly broad peak with a larger amount of hybridized metal-*d* carbon-*p*, containing exactly 2 states, is filled when going to MoC while in the other structures the region filled is with more metal-*d* character with a smaller amount of carbon-*p*. The stability of the WC structure is not much changed when going from ZrC to MoC, see the discussion about formation energies in Sec. III and cohesive energies in Sec. V. This shows that the states of the broad peak in the DOS above the Fermi level (which is filled in the MoC case) for the WC structure of ZrC is comprised of slightly stabilizing states that are slightly bonding/nonbonding while the destabilizing states above the Fermi level being filled in the other structures are mostly antibonding. For TcC the WC structure is no longer stable having now filled antibonding electronic states above the slightly bonding/nonbonding peak.

B. DOS of substoichiometric cubic MeC_{1-x}

In Fig. 10 the calculated partial density of states for 5 different vacancy concentrations of cubic ZrC_{1-x} are displayed and the trends and changes in the DOS are clearly seen when introducing vacancies in the carbon sublattice. This DOS is representative of all three substoichiometric carbides, the DOS of the other two, NbC_{1-x} and MoC_{1-x} being qualitatively the same. The only major difference in the DOS between the three carbides at each stoichiometry can be understood in terms of a simple rigid band filling. The approximate position of the Fermi level in NbC_{1-x} and MoC_{1-x} is indicated in the DOS for ZrC_{1-x}. Note that when removing atoms in the carbon sublattice the symmetry of the system is changed and therefore there is more than one type of Me atom in these systems. For sake of clarity only the partial density of states of one of these is displayed, the others being qualitatively similar to the one displayed or not significantly changed from the MeC case (for those atoms not having carbon vacancies as neighbors).

The topmost plot of Fig. 10 displays stoichiometric cubic MeC, as seen previously in Fig. 9. Below this plot the DOS for $MeC_{0.75}$ is shown where regions I and II remain largely unchanged, with the peak in region II becoming lower and more narrow. The largest changes are found in region III where the minimum which separated regions II and III is now pierced by two peaks with mostly Me-*d* character. These peaks are the so-called vacancy peaks and are associated with unscreened Me-Me bonds through the vacancy site and have been more extensively studied in our previous

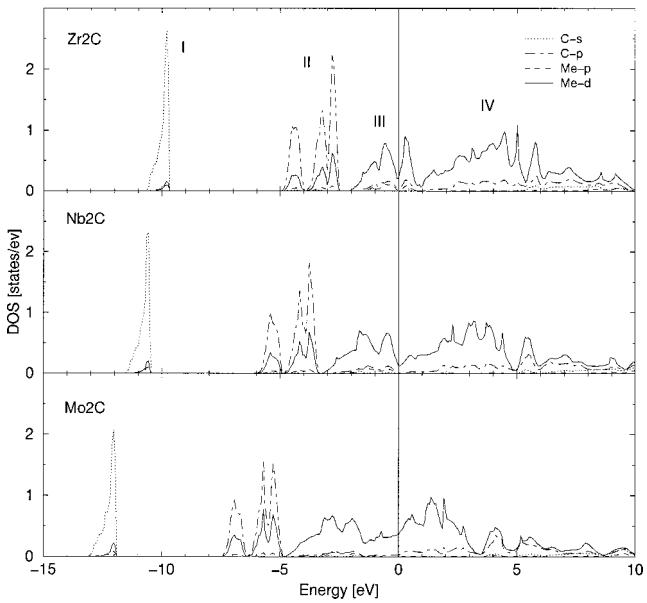

FIG. 11. Density of states for the hexagonal Me_2C phases for Zr_2C, Nb_2C, and Mo_2C. The Fermi level is indicated by a solid line.

work.[14] The Fermi level of $ZrC_{0.75}$ is between the two peaks, for $NbC_{0.75}$ it is found on the first peak and in $MoC_{0.75}$ above both vacancy peaks.

Starting from the top-most DOS for MeC and proceeding downwards the DOS is gradually changed from a clear hybridization between Me-*d* and C-*p*, with emergence of vacancy peaks in the 25% vacancy case. These vacancy peaks become more and more pronounced at 50% and at 75%, until in the pure transition metal the *d*-band is seen in the lowest picture. The Fermi level is also lowered from high up in the *d*-band towards the center of the *d*-band for the pure fcc metal. It is also clear that the inclusion of vacancies in the carbon sublattice cannot be viewed in a rigid band filling picture and for all the MeC_{1-x} compounds the Fermi level is fairly inert, giving more a picture of *plastic bands* were the vacancies drastically changes the nature of the bonding.

C. Electronic structure of the Me_2C phases

The DOS for the hexagonal Me_2C phases for Zr_2C, Nb_2C and Mo_2C are shown in Fig. 11. For clarity of discussion the DOS can be divided into four main regions (indicated in the topmost part of Fig. 11). The main features in the electronic structure is a low sharp peak with C-*s* character hybridized with Me-*d* at around -10 eV in region I followed by region II containing 6 electrons comprised of strongly hybridized C-*p* and Me-*d* electronic states above -5 eV. The electronic states around the Fermi level, region III, are mainly Me-*d* and a small part C-*p* and Me-*p* containing 6 states while the higher energy region IV is only Me-*d* and C-*p*.

As for the previously studied phases the difference between the DOS of hexagonal Zr_2C and hexagonal Nb_2C/Mo_2C is seen to be mostly a rigid band shift of the Fermi level. The main differences in the bonding between the compounds is seen to be that there is an increased hybridization between the C-*p* and metal-*d* states in region II when going from Zr_2C to Mo_2C. The stabilization by the increase of hybridization is however negated by an increased filling of the states in region III. Combining results from the discussion on energies of formation in Sec. III C and cohesive energies in Sec. V, the last part of region III, from -2 eV to 1 eV which is filled in hexagonal Nb_2C, is of a destabilizing but bonding nature. The states above 1 eV in region IV, filled in hexagonal Mo_2C, are nonbonding but less bonding than the states in the individual elements and thus destabilizing.

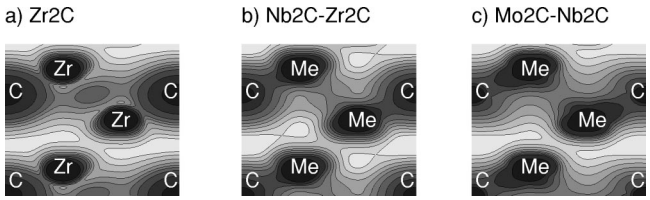

FIG. 12. Charge density contours from the electronic states in region II (as indicated in Fig. 11) seen in the [2 4 3] plane. The regions inside the dark contours have more electron density than those inside lighter contours. Figure (a) shows the total charge density for Zr_2C while figures (b) and (c) show the difference in charge density for this region when Zr is exchanged for Nb and Mo, respectively.

As discussed above, a closer study of the DOS for the hybridized Me-*d* C-*p* states in region II indicates that the degree of hybridization is increased when going from Zr_2C to Mo_2C. Figure 12 shows the charge density originating from region II in a [2 4 3] plane of the crystal. The left-most figure, Fig. 12(a), shows the charge density from region II in Zr_2C while the next two figures, Figs. 12(b) and 12(c) show the difference in charge density when going to Nb_2C and Mo_2C, respectively. Fig. 12(a) clearly shows the very layered nature of the bonds in region II, where all the charge is in bonds between metal and nonmetal atoms and even some bonding between carbon neighbors is seen (the charge seen between the top two metal atoms). Figures 12(b) and 12(c) then clearly show that the difference in bonding when going to Nb_2C and Mo_2C is that more charge is placed in the metal to nonmetal bonds. This is due to an increase in the *p*-*d* hybridization as indicated from the changes in the DOS. The distribution of total charge densities have also been studied for a plane in the crystal indicating the very layered nature of the bonding in the hexagonal Me_2C phases.

The DOS of orthorhombic Mo_2C is shown in Fig. 13. The main differences between the DOS for the hexagonal and the orthorhombic Mo_2C phases is that there is no gap between the strongly hybridized Mo-*d* C-*p* states in region II and the Mo-*d* states in region III. The strongly hybridized states in region II are also found to be situated lower in energy for the orthorhombic structure thereby correctly indicating that this structure is more stable than the hexagonal structure.

VII. CONCLUSIONS

The results of this study of the phase stabilities and homogeneity ranges of the 4*d*-transition-metal carbides can be summarized in seven points.

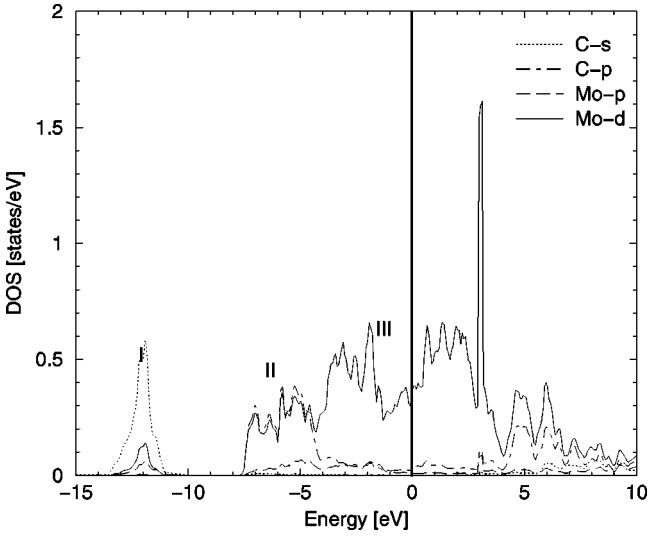

FIG. 13. Density of states for orthorhombic Mo_2C. The Fermi level is indicated by a solid line.

(i) Theoretical zero temperature phase stability diagrams have been calculated for the $4d$-transition-metal carbides. Calculation of the energies of formation of the competing hexagonal Me_2C phases explains the differences found in homogeneity ranges and equilibrium composition for the substoichiometric cubic MeC_{1-x} phases. The values of the formation energy and equilibrium volumes should also be of interest as input in other theoretical schemes for constructing phase diagrams.

(ii) The variation in the homogeneity range of the substoichiometric cubic carbides can be understood from the phase diagrams as arising from the differences in electronic structure with the deoccupation of stabilizing and destabilizing electronic states when vacancies are introduced to the structure. These differences couple into two separate mechanisms where the variation stems from either a competition between the substoichiometric cubic phase and the Me_2C phases plus graphitic carbon or from a competition with stoichiometric MeC plus pure metal Me. The range in where the substoichiometric carbide is more stable than both these determines the homogeneity range.

(iii) From the changes in formation energy it is indicated that the states that are filled when going from ZrC to MoC in the hexagonal WC structure are nonstabilizing/stabilizing (since E_{form} is fairly constant) up to MoC and then destabilizing (E_{form} increases). In the other three structures, among them the cubic NaCl structure, all the states filled when traversing the series from ZrC to MoC are mostly destabilizing. The WC-structure is therefore seen to become the most stable structure for MoC not by becoming more stable but because the other phases are destabilized. This picture is also supported by studies of the electronic structure.

(iv) The order of stability for the four MeC phases, found in MoC, was calculated for ZrC, NbC, and MoC (and TcC). The changes in relative phase stability was explained by differences in the filling of states in the electronic structure.

(v) The combined results from the studies of the cohesive energies and energies of formation indicate that the region of maximal stability of the phases is shifted from the beginning of the series (Zr) for the transition-metal carbides towards the middle (Mo, Tc) when increasing the metalization via the transition-metal hemicarbides to the pure metals. It is thus concluded that carbides Me_xC, $x>1$, should be more prevalent closer to the middle of the series, obtained for example by alloying.

(vi) Theoretical equilibrium structures for the hexagonal Me_2C phases have been calculated, showing good agreement with experiment. Studies of the electronic structure in these hexagonal phases show a very layered bonding.

(vii) The electronic structures and stabilities of the experimentally reported orthorhombic Nb_2C and Mo_2C phases have also been studied. The two reported orthorhombic structures of Nb_2C were found to be less stable than the hexagonal phase. The stability of the orthorhombic Mo_2C phase was greater than the hexagonal phase, in agreement with experiment.

ACKNOWLEDGMENTS

This work has been supported by the Swedish Research Council (NFR and TFR) and the Swedish Foundation for Strategic Research (SSF). Dr. J. M. Wills of Los Alamos National Laboratories is acknowledged for supplying the FP-LMTO code used in these studies.

[1] Several experimental phase diagrams exist; the ones used in this article have been taken from *Binary Alloy Phase Diagrams*, edited by T. B. Massalski (ASM International, Materials Park, OH, 1990).

[2] The metastable γ'-MoC (TiAs) phase was previously thought to be stable only after the inclusion of oxygen. The phase has, however, recently been shown to be a true metastable MoC phase. J. Lu, H. W. Hugosson, O. Eriksson, L. Nordström, and U. Jansson, Thin Solid Films **370**, 203 (2000).

[3] J.L. Calais, Adv. Phys. **26**, 1847 (1977).

[4] A. Neckel, Int. J. Quantum Chem. **XXIII**, 1317 (1983).

[5] K. Schwarz, CRC Crit. Rev. Solid State Mater. Sci. **13**, 211 (1987).

[6] L. I. Johansson, Surf. Sci. Rep. **21**, 177 (1995).

[7] D. L. Price and B. R. Cooper, Phys. Rev. B **39**, 4945 (1989).

[8] A. L. Ivanovskii, V. I. Anisimov, and V. A. Gubanov, J. Struct. Chem. **30**, 184 (1989).

[9] V. V. Krainik, A. A. Lisenko, V. I. Ivaschenko, and V. L. Bekenev, Dokl. Akad. Nauk (SSSR) **307**, 1365 (1989) [Sov. Phys. Dokl. **34** (8), 722 (1989)].

[10] J. Redinger, R. Eibler, P. Herzig, A. Neckel, R. Podloucky, and E. Wimmer, J. Phys. Chem. Solids **46**, 383 (1985).

[11] J. Redinger, R. Eibler, P. Herzig, A. Neckel, R. Podloucky, and E. Wimmer, J. Phys. Chem. Solids **47**, 387 (1986).

[12] W. Wolf, R. Podloucky, T. Antretter, and F. D. Fischer, Philos. Mag. B **79**, 839 (1999).

[13] A. L. Ivanovskii, V. I. Anisimov, D. L. Novikov, A. I. Lichtenstein, and V. A. Gubanov, J. Phys. Chem. Solids **49**, 465 (1988).
[14] H. W. Hugosson, O. Eriksson, L. Nordström, U. Jansson, L. Fast, A. Delin, J. M. Wills, and B. Johansson, J. Appl. Phys. **86**, 3758 (1999).
[15] V. Ozolins and J. Häglund, Phys. Rev. B **48**, 5069 (1993).
[16] M. H. F. Sluiter and Y. Kawazoe, Modell. Simul. Mater. Sci. Eng. **8**, 221 (2000).
[17] J. M. Wills, O. Eriksson, and M. Alouani, in *Electronic Structure and Physical Properties of Solids*, edited by Hugues Dreysse (Springer-Verlag, Berlin, 2000), p. 148.
[18] H. Skriver, *The LMTO Method*, Solid State Sciences (Springer-Verlag, Berlin, 1984).
[19] L. Hedin and B.I. Lundqvist, J. Phys. C **4**, 2064 (1971).
[20] M. Methfessel and A. T. Paxton, Phys. Rev. B **40**, 3616 (1989); J. M. Wills, O. Eriksson, P. Söderlind, and A. M. Boring, Phys. Rev. Lett. **68**, 2802 (1990).
[21] This was checked for different stoichiometries and the effect on the equilibrium volumes was small.
[22] The effect of local relaxations around the vacancy, as opposed to the total relaxation of the whole lattice, has been studied in some previous works, like for example a recent study of monovacancies in transition metals due to P. Söderlind and co-workers (Ref. 35). The magnitude of the local relaxation depends on the supercell size used, the larger the supercell the more of the relaxation is local, around the vacancy, and less is in overall relaxation of the lattice. With the supercells used in this study most of the vacancy relaxation will take place as a ''global'' relaxation of the lattice parameter. Therefore we do not expect, based upon our experience with related systems (TiC_{1-x}) (Ref. 36), that the inclusion of local relaxation should lower the formation energies with more than a few mRy. Similarly, the density of states for the locally relaxed structures has also been seen, in a study of substoichiometric cubic TiC_{1-x}, not to be much changed from that of the unrelaxed structure (Ref. 36).
[23] This has also been addressed in one of our earlier works where the stability of the phases was compared between MoC and WC. There it was also seen that the energy differences between the two most stable phases in WC, the WC and TiAs structures, was almost twice that in MoC (Ref. 14).
[24] The C atoms are removed in such a fashion that a stoichiometric Me_2C phase with ''striped'' vacancy structures reported for Ti_2C is reached. P. Wanjara, R. A. L. Drew, J. Root, and S. Yue, Acta Mater. **48**, 1443 (2000).
[25] The experimental c/a of Nb_2C is 1.572.
[26] The calculated lattice parameters are slightly smaller; this is a well-known effect of LDA. LDA tends to ''overbind.''
[27] The space group of orthorhombic Nb_2C was reported by Yvon, Nowotny, and Keiffer (Ref. 37) to be C^9_{2v}-$Pnma$. This must however be a mistake since $Pnma$ is D^{16}_{2h}. The position of the atoms in the $Pnma$ structure is not compatible with those given in the article, so C^9_{2v} (being $Pna2_1$) was used in our study. A second orthorhombic structure, with the same lattice parameters as for the orthorhombic structure reported by Yvon *et al.*, is reported by Khaenko and Gnitetskii (Ref. 38). The space group was here found to be Pm. A third space group for the orthorhombic Nb_2C structure is proposed in Pearsons Handbook, also being attributed to Yvon *et al.* (1967), now being $Pmc2_1$ (Ref. 39). This is once again clearly erroneous since the distance between the atoms in this case would be less than 1 Å. In our study we have calculated the properties of two orthorhombic Nb_2C structures; first using the C^9_{2v} ($Pna2_1$) space group and secondly using the atomic positions reported by Khaenko and Gnitetskii (Ref. 38).
[28] The experimental lattice parameters are $a=4.724$, $b=6.004$, and $c=5.199$. E. Parthe and V. Sadagopan, Acta Crystallogr. **16**, 202 (1963).
[29] It has been found in a study of substoichiometric titanium carbide that in order to obtain the correct experimental composition for the substoichiometric transition metal carbides one must also include the effect of local relaxations of the atoms around the vacancies (Ref. 36).
[30] J. Friedel, in *The Physics of Metals*, edited by J.M. Ziman (Cambridge University Press, New York, 1969); W. Harrison, *Electronic Structure and the Properties of Solids* (Freeman, San Francisco, 1980).
[31] C. D. Gelatt, A. R. Williams, and V. L. Moruzzi, Phys. Rev. B **27**, 2005 (1983).
[32] M. S. S. Brooks, J. Phys. F **13**, 103 (1983).
[33] H. W. Hugosson, L. Nordström, U. Jansson, B. Johansson, and O. Eriksson, Phys. Rev. B **60**, 15 123 (1999).
[34] The equilibrium c/a for these structures was found to be ZrC(WC): 0.92, NbC(WC): 0.96, MoC(WC): 0.97, ZrC(TiAs): 3.57, NbC(TiAs): 3.57, MoC(TiAs): 3.74, ZrC(η): 4.86, NbC(η): 4.93, and MoC(η): 5.08.
[35] P. Söderlind, L. H. Yang, J. A. Moriarty, and J. M. Wills, Phys. Rev. B **61**, 2579 (2000).
[36] H. W. Hugosson, P. Korzhavyi, U. Jansson, B. Johansson, and O. Eriksson, Phys. Rev. B (to be published).
[37] K. Yvon, H. Nowotny, and R. Keiffer, Monatsh. Chem. **98**, 34 (1967).
[38] B. V. Khaenko and O. A. Gnitetskii, Kristallografiya **38**, 55 (1993) [Crystallogr. Rep. **38**, 741 (1993)].
[39] P. Villars and L. D. Calvert, *Pearsons Handbook of Crystallographic Data for the Intermetallic Phases* (American Society for Metals, Metals Park, OH, 1985).